ACS Energy LETTERS

http://pubs.acs.org/journal/aelccp

Rational Electrolyte Design to Form Inorganic–Polymeric Interphase on Silicon-Based Anodes

Shaoxiong Yang,[⊥] Yuping Zhang,[⊥] Zhongliang Li, Norio Takenaka, Yan Liu, Hanqin Zou, Wenting Chen, Mingcong Du, Xu-Jia Hong, Rui Shang, Eiichi Nakamura, Yue-Peng Cai, Ya-Qian Lan, Qifeng Zheng,* Yuki Yamada, and Atsuo Yamada*

Cite This: *ACS Energy Lett.* 2021, 6, 1811−1820

Read Online

ACCESS | Metrics & More | Article Recommendations | Supporting Information

ABSTRACT: Silicon-based materials have been regarded as the most promising anodes for high-energy batteries, when combined with high- voltage/capacity nickel-rich layered cathodes. However, challenges arise from unstable electrode/electrolyte interphases on the anode and cathode as well as from safety hazards associated with highly flammable commercial electrolytes. Herein, we rationally design a nonflammable cyclic phosphate-based electrolyte to tune the electrode/electrolyte interphase components by controlling the reduction of a cyclic phosphate and Li salt. This strategy enables the electrolyte to form a highly elastic, robust inorganic−polymeric interphase on microsized silicon-based anodes that can accommodate the immense volume changes. Furthermore, by generating a stable polymeric interphase on the surface of the cathode as well, a Si|O|$LiNi_{0.6}Mn0.2Co_{0.2}O_2$ cell demonstrated an extremely high energy density of ∼590 Wh·kg^{-1} with 71.4% capacity retained over 300 cycles and high Coulombic efficiency of 99.9%. This interfacial regulation strategy is of vital importance for designing new electrolytes for high-energy-density batteries.

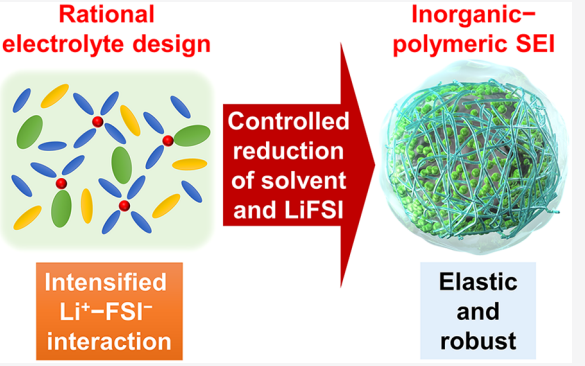

Lithium-ion batteries (LIBs) have dominated consumer electronics because of their high energy densities and long-term cycle lives.[1,2] To fulfill the energy storage demand for massive applications like electric vehicles, increasing the energy density of LIBs is desperately needed, which largely relies on the use of high- voltage/capacity cathodes, high-capacity anodes, and compatible electrolytes.[3−5]

In recent years, tremendous efforts have been devoted toward exploring high- voltage/capacity cathode materials,[6−8] such as $LiCoPO_4$, $LiCoMnO_4$, $LiNi_{0.5}Mn_{1.5}O_4$, and especially $LiNi_xMn_yCo_zO_2$ (NMC, $x + y + z = 1$) layered oxides, where NMC has been considered as the most promisingreplacement for $LiCoO_2$ because of its high capacity and favorable electrochemical stability.[7] Particularly, Ni-rich NMC ($x \geq 0.5$) cathodes with high Ni and low Co content,[7,9] such as $LiNi_{0.6}Mn_{0.2}Co_{0.2}O_2$ (NMC622) and $LiNi_{0.8}Mn_{0.1}Co_{0.1}O_2$ (NMC811), contribute to an increased capacity and reduced cost and have thus attracted a great deal of attention in both academia and industry. Furthermore, a significantly higher capacity could be achieved by elevating the cutoff voltage. For instance, the discharge capacity of the NMC622 cathode has often been reported to exceed 200 mAh g^{-1} when charged to over 4.6 V.[10,11] Unfortunately, Ni-rich NMC cathodes generally suffer from structural and thermal instabilities that lead to poor cycling performance and fire accidents, and these problems worsen at higher cutoff voltages.[7,9] In addition, high-voltage operation does not exclusively depend on the features of the cathode material but also largely on the electrolyte. The conventional carbonate-based electrolyte is anodically unstable when charged over 4.4 V, causing solvent decomposition and transition-metal dissolution from the cathode and resulting in significant capacity fading.[12,13]

As for high-capacity anodes, silicon (Si)-based materials are the most promising replacement because of their high theoretical capacities and low operating potentials (i.e., ∼0.2 V versus Li/Li^+).[14−17] However, Si-based anodes experience

Received: March 10, 2021
Accepted: April 12, 2021
Published: April 15, 2021

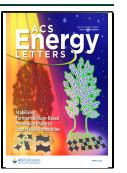

https://doi.org/10.1021/acsenergylett.1c00514
ACS Energy Lett. 2021, 6, 1811−1820

Scheme 1. Safe Electrolyte Design for High-Capacity Si-Based Anodes[a]

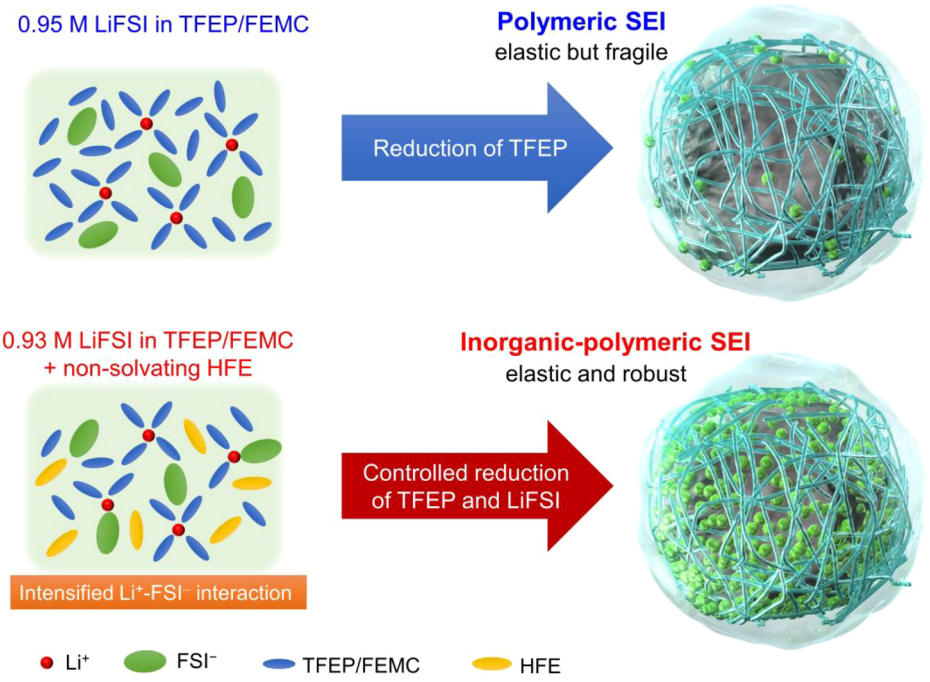

[a]Reduction of a fluorinated cyclic phosphate (i.e., TFEP) forms a highly elastic polymeric SEI. To increase the mechanical toughness of the polymeric SEI, a non-solvating hydrofluoroether (i.e., HFE) is introduced, which intensifies the Li^+−FSI^- association and promotes the reduction of FSI^-, thereby generating additional FSI^- anion-derived inorganic components and leading to a highly elastic and robust inorganic−polymeric SEI.

immense volume expansion and shrinkage upon cycling, which cause mechanical fracture of the anode particles, loss of electric contact, and excessive growth of the solid-electrolyte interphase (SEI), leading to a low cycling Coulombic efficiency (CE) and poor cycling life.[17−19] Intensive research has been dedicated to addressing these issues. For instance, various nanostructured Si-based materials,[15−17,19−21] such as nanowires, nanoparticles, nanocomposites, and core−shell structures, have been shown to effectively enhance the battery performance in half-cells. However, the complicated preparation processes, high costs, and low CEs associated with nanostructured designs make these strategies inadequate for industrial applications. Furthermore, various functional binders[22−25] with superelasticity and self-healing properties have demonstrated their capability to alleviate the pulverization and maintain the integrity of Si-based electrodes. Unfortunately, the use of solely functional binders generally cannot meet the industrial requirements for practical applications.[22]

Therefore, in addition to these electrode treatments, many research efforts toward electrolytes and additives have also been carried out to further boost the CEs and capacity retentions.[22,26,27] Vinylene carbonate (VC) and fluoroethylene carbonate (FEC) are the most well-known and studied additives for Si-based anodes in LIBs because they significantly enhance the cycling performance.[28−31] Nevertheless, the SEI generated by FEC or VC is not robust enough to bear the immense volume changes of Si-based anodes, especially for microsized samples, and thus yield unsatisfactory CEs (i.e., < 99.8%) during cycling.[32,33] Very recently, Wang's group[34] formulated a 2.0 mol dm^{-3} (M) $LiPF_6$−mixed tetrahydrofuran (THF) electrolyte that forms an LiF−organic bilayer SEI on microsized Si anodes, enabling 400 stable cycles with a CE of >99.9%. However, the poor oxidative stability of THF above 4.2 V will largely hinder the application of this electrolyte to high-voltage cathodes. Furthermore, the low boiling points and high flammability of THF, as well as conventional carbonate-based electrolytes, may give rise to additional safety issues under certain extreme conditions.[35−37] Therefore, it is in high demand to develop a highly oxidative-stable and nonflammable electrolyte that can form a robust SEI to hold the immense volume changes of Si-based anodes, as well as an effective cathode electrolyte interphase (CEI) to inhibit the structural collapse and transition-metal dissolution of high-voltage/capacity cathodes.

Herein, we report a new electrolyte design strategy in tuning SEI components that allows for the stable operation of Si-based electrodes in a nonflammable electrolyte, which is formulated by dissolving 0.93 M lithium bis(fluorosulfonyl)-imide (LiFSI) in a mixture of 2-(2,2,2-trifluoroethoxy)-1,3,2-dioxaphospholane 2-oxide (TFEP)/2,2,2-trifluoroethyl methyl carbonate (FEMC)/1,1,2,2-tetrafluoroethyl 2,2,3,3-tetrafluoropropyl ether (HFE) (1:3:1 by volume). As shown in Scheme 1, the fluorinated cyclic phosphate (i.e., TFEP) solvent contributes to the formation of a highly elastic polymeric interphase, and the nonsolvating hydrofluoroether (i.e., HFE)[38] intensifies the Li^+−FSI^- association. This facilitates the formation of additional FSI^- anion-derived inorganic interphase that is mechanically robust, thus building a highly elastic and robust inorganic−polymeric SEI. Furthermore, the stable operation of Ni-rich NMC622 cathodes and SiO| NMC622 full cells at a high cutoff voltage was realized with the proposed strategy owing to the efficient prevention of electrolyte oxidation, Al corrosion, and transition-metal dissolution.

Conventional carbonate-based electrolytes are highly flammable therefore usually give rise to fire accidents.[35,39] Organic

https://doi.org/10.1021/acsenergylett.1c00514
ACS Energy Lett. 2021, 6, 1811−1820

phosphates, such as trimethyl phosphate and hexamethylphosphoramide, are recognized for their nonflammable characteristics because phosphorus can act as a trapping agent for hydrogen radicals.[40,41] Unfortunately, linear organic phosphates fail to generate a valid SEI on the anode (e.g., graphite or Si-based anodes), leading to poor battery performance; thus, they have been excluded from battery electrolytes unless employed in high concentrations.[42] Very recently, we synthesized a fluorinated cyclic phosphate solvent molecule, TFEP, which has both intrinsic nonflammability and excellent SEI-forming capability on graphite anodes.[43] In addition to some inorganic species, the SEI formed by this cyclic phosphate-based electrolyte mainly consists of polyphosphoesters, a type of elastomer that is highly elastic,[44] which may be able to accommodate the significant volume changes of Si-based electrodes.

To enhance the mechanical strength of the TFEP-derived SEI, a nonsolvating hydrofluoroether (i.e., HFE)[45] was employed as a cosolvent. HFE was expected to increase the fraction of contact ion pairs (CIPs) and aggregates (AGGs) of LiFSI, thereby inducing the contribution of FSI^- anions to the SEI[46] (Scheme 1). The optimized electrolyte is composed of 0.93 M LiFSI salt in a mixed solvent of TFEP, FEMC, and HFE (1:3:1 by volume) to maintain an identical salt-to-solvent molar ratio of 1:8 (0.93 M LiFSI in TFEP/FEMC/HFE). Because we maintained a salt-to-solvent (all solvent) molar ratio at 1:8 for both cyclic phosphate-based electrolyte, which makes the LiFSI: TFEP: FEMC: HFE molar ratio 1:1.58:5.06:1.36 in 0.93 M LiFSI in TFEP/FEMC/HFE electrolyte and the LiFSI: TFEP: FEMC molar ratio 1:1.90:6.10 in 0.95 M LiFSI in TFEP/FEMC electrolyte.

Indeed, the Raman band at 1210−1230 cm^{-1} matching to the coordination states of the FSI^- anion[47] shifted to a higher wavenumber with the addition of HFE (Figure S1), which suggests that the Li^+-FSI^- association was intensified as a result of the accumulation of CIPs and AGGs. In these ion-paired states, the electron of the FSI^- is partially donated to Li^+, which may raise the reduction potential of FSI^- and thereby promote its reductive decomposition to produce additional FSI^- anion-derived inorganic interphase.[46] Together with the highly elastic polymeric component offered by TFEP, a highly elastic and robust inorganic−polymeric SEI could be realized that can sustain the stable cycling of Si-based anodes.

Oxidative stability is the most important criterion in designing electrolytes for high-voltage cathodes. Of TFEP, FEMC, and HFE as the employed solvents and ethylene carbonate (EC), ethyl methyl carbonate (EMC), and dimethyl carbonate (DMC) as common electrolyte solvents, HFE has the highest oxidative stability according to the density functional theory (DFT) calculations (Table S1). Furthermore, as has been demonstrated in locally concentrated electrolytes with diluent HFE,[48−50] the nonsolvating HFE would also strengthen the coordination of TFEP and FEMC to Li^+, thus further enhancing their oxidative stability. Linear sweep voltammetry (LSV) was employed to study the oxidative stability of the electrolyte (Figure S2). A dramatic oxidation current at 4.4 V was observed for 1 M $LiPF_6$ in EC/DMC, corresponding to oxidative decomposition of the carbonate solvents. The oxidation potentials were postponed to ∼ 4.9 V for the 0.95 M LiFSI in TFEP/FEMC and further improved to ∼5.1 V for the 0.93 M LiFSI in TFEP/FEMC/HFE electrolyte, which was attributed to fluorine substitution (i.e., −F and $-CF_3$) significantly lowering the highest occupied molecular orbitals (HOMOs) of the solvents (Table S1),[51] as well as the diluent effect of HFE.

To elucidate the effect of the HFE cosolvent on the solvation structure, two cyclic-phosphate-based electrolytes, namely, 0.95 M LiFSI in TFEP/FEMC (60LiFSI + 114TFEP + 366FEMC) and 0.93 M LiFSI in TFEP/FEMC/HFE (60LiFSI + 95TFEP + 304FEMC + 82HFE), were studied by molecular dynamics (MD) simulations (Figure 1). The radial

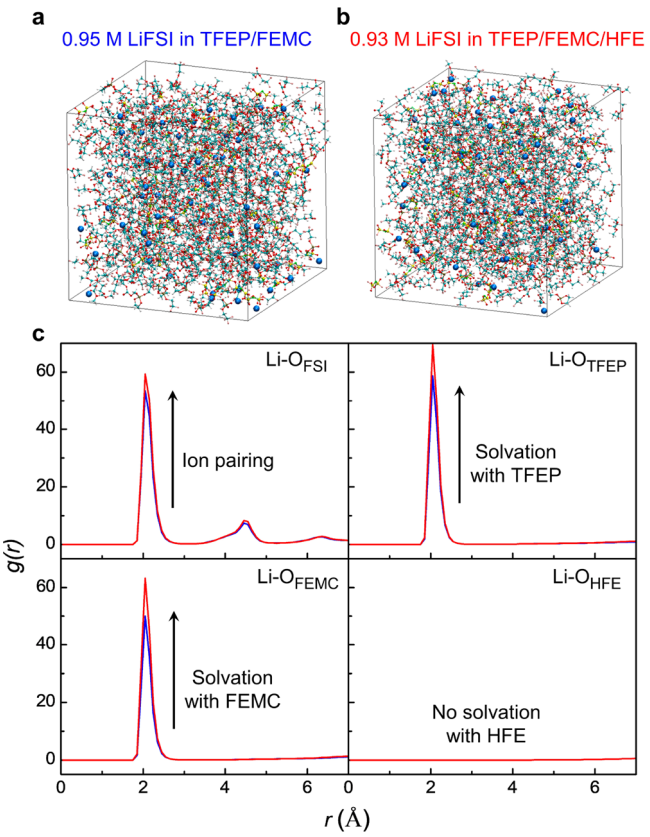

Figure 1. Theoretical studies of solvation structures. MD simulation snapshots of (a) 0.95 M LiFSI in TFEP/FEMC and (b) 0.93 M LiFSI in TFEP/FEMC/HFE electrolytes at 298 K. (c) Radial distribution functions $g(r)$ of $Li-O_{FSI}$, $Li-O_{TFEP}$, $Li-O_{FEMC}$, and $Li-O_{HFE}$ pairs calculated from MD simulations at 298 K in the two electrolytes. Compared with 0.95 M LiFSI in TFEP/FEMC, adding the HFE cosolvent not only promotes the formation of Li^+-FSI^- ion pairs, which may contribute to additional FSI^- anion-derived inorganic interphase, but also promotes the coordination of both TFEP and FEMC to Li^+, which enhances the oxidative stability.

distribution functions of the $Li-O_{FSI}$, $Li-O_{TFEP}$, $Li-O_{FEMC}$, and $Li-O_{HFE}$ pairs were calculated and are shown in Figure 1c. A distinct peak for Li−O was assigned at 2.05 Å for the $Li-O_{FSI}$, $Li-O_{TFEP}$, and $Li-O_{FEMC}$ pairs in both cyclic phosphate-based electrolytes, for which the peak intensities were stronger in the presence of HFE (i.e., 0.93 M LiFSI in TFEP/FEMC/HFE). Meanwhile, HFE was found to barely coordinate with Li^+, demonstrating its nonsolvating feature. Notably, the coordination number of FSI^- anion (the first coordination sphere of oxygen) increased from 2.20 to 2.33 with the addition of HFE, which agrees well with the experimental trend of higher wavenumber in the Raman spectra (Figure S1). This clearly indicates that the addition of nonsolvating HFE not only promotes the ion pairing of Li^+-FSI^-, which may

https://doi.org/10.1021/acsenergylett.1c00514
ACS Energy Lett. 2021, 6, 1811−1820

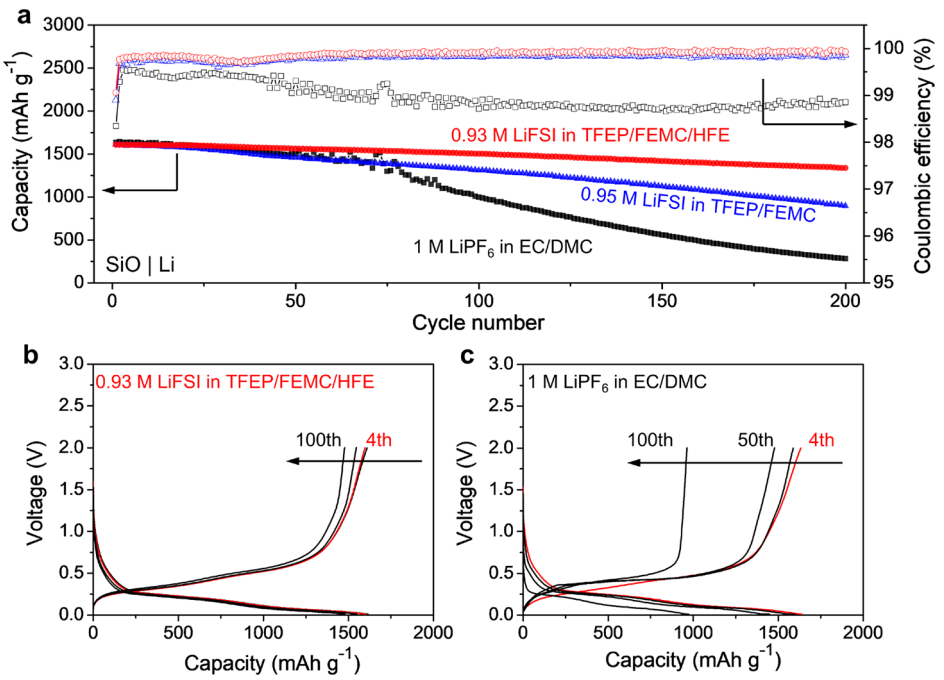

Figure 2. Electrochemical performance of SiO electrodes. (a) Cycling performance of the SiO|Li half-cells using 0.93 M LiFSI in TFEP/FEMC/HFE, 0.95 M LiFSI in TFEP/FEMC, and 1 M $LiPF_6$ in EC/DMC at 0.2 C after three formation cycles at 0.05 C. Selected charge−discharge curves for the half-cells at 0.2 C with (b) 0.93 M LiFSI in TFEP/FEMC/HFE and (c) 1 M $LiPF_6$ in EC/DMC. The first charge−discharge curves are shown in Figure S6.

contribute to additional FSI^- anion-derived inorganic interphase, but also promotes the coordination of both TFEP and FEMC to Li^+ that enhances their oxidative stability (Figure S2). This further supports our electrolyte design rationale for simultaneously realizing a robust interphase and high oxidative stability.

Si-based (i.e., SiO or Si) electrodes with a particle size of 1−5 μm were used to investigate the electrochemical performance of various electrolytes. Polyamide imide (PAI), which has been reported to provide better interfacial adhesion, was chosen as binder for Si-based electrode. As shown in Figure S6, the SiO|Li cell using 0.93 M LiFSI in TFEP/FEMC/HFE delivered an initial capacity of ~1680 mAh g^{-1} with a CE of 79.0% at 0.05 C, which is slightly higher than those obtained using 0.95 M LiFSI in TFEP/FEMC and 1 M $LiPF_6$ in EC/DMC (77.1% and 74.7%, respectively). Furthermore, as shown in Figure 2, the SiO|Li cell with 0.93 M LiFSI in TFEP/FEMC/HFE retained 83.1% capacity over 200 cycles at 0.2 C with a high average CE of ~99.9%, which exceeds those obtained with 0.95 M LiFSI in TFEP/FEMC (~99.8%) and 1 M $LiPF_6$ in EC/DMC (98.8%). Furthermore, as shown in Figure S8, even with 5 vol % FEC as additive in 1 M $LiPF_6$ in EC/DMC, the SiO|Li cell retained only 31.8% capacity over 200 cycles with highly fluctuated CE, indicating unstable interphase on the micro-sized SiO particles that are more prone to mechanical failure. In addition, the SiO|Li cell with 0.93 M LiFSI in TFEP/FEMC/HFE also showed decent rate performance, as 47.7% capacity was maintained at 2 C (Figure S9).

The composition of the SEI is of vital importance for the electrochemical performance of SiO electrodes and was thus carefully investigated by X-ray photoelectron spectroscopy (XPS) (Figure 3a). The SEI formed from 1 M $LiPF_6$ in EC/DMC was mainly composed of Li-carbonate (Li_2CO_3), Li-alkyl carbonates ($ROCO_2Li$), and Li-alkoxides (ROLi) resulting from EC reduction.[52] As has been widely demonstrated in previous studies[26,27] and by our results (Figure 2), such an EC-derived SEI is unstable and too rigid to tolerate the volumetric stress during delithiation (Figure 3b), leading to its rupture and breakdown into separate pieces. Thereafter, fresh SiO surface is exposed to the electrolyte, causing continuous growth and thickening of the SEI and consumption of the electrolyte,[26,32] as evidenced by both transmission and scanning electron microscopy (TEM and SEM) images (Figures 3d and S10b) acquired after 100 cycles. Furthermore, the TEM EDS mapping images show that the pulverized SiO is enveloped in a thick SEI containing elements mainly of C and O (Figure S11a).

As for the SiO electrodes in 0.95 M LiFSI in TFEP/FEMC and 0.93 M LiFSI in TFEP/FEMC/HFE, a sharp peak at 684.9 eV corresponding to LiF was present in the F 1s spectra. LiF, with its low electronic conductivity, large bandgap, and high electrochemical stability, has been proposed to be an excellent SEI component for various anodes, such as graphite,[47] silicon,[34] and Li metal.[53] Furthermore, the O 1s spectra showed a clear peak at 528.3 eV corresponding to lithium oxide (Li_2O), which may be generated by TFEP or LiFSI and could serve as a buffer component to sustain the volume changes upon cycling.[54] Characteristic peaks corresponding to CF_3 were detected in both the C 1s and F 1s spectra. P-containing compounds (i.e., PO_y) were detected in the P 2p spectra, which could be assigned to Li_xPO_y and polyphosphoesters. This is consistent with the electrospray ionization−quadrupole time-of-flight mass spectrometry (ESI-Q-TOF-MS) results, of which the phosphate oligomer species are indentified as SEI components (Figure S12 and Table S2). On this basis, we assume that TFEP is reduced to produce LiF, Li_2O, Li_xPO_y, and polyphosphoesters. To the best of our knowledge, this is the first finding of such an SEI derived from a nonflammable phosphate solvent that can sustain the stable cycling of Si-based electrodes with a reasonably high CE

https://doi.org/10.1021/acsenergylett.1c00514
ACS Energy Lett. 2021, 6, 1811−1820

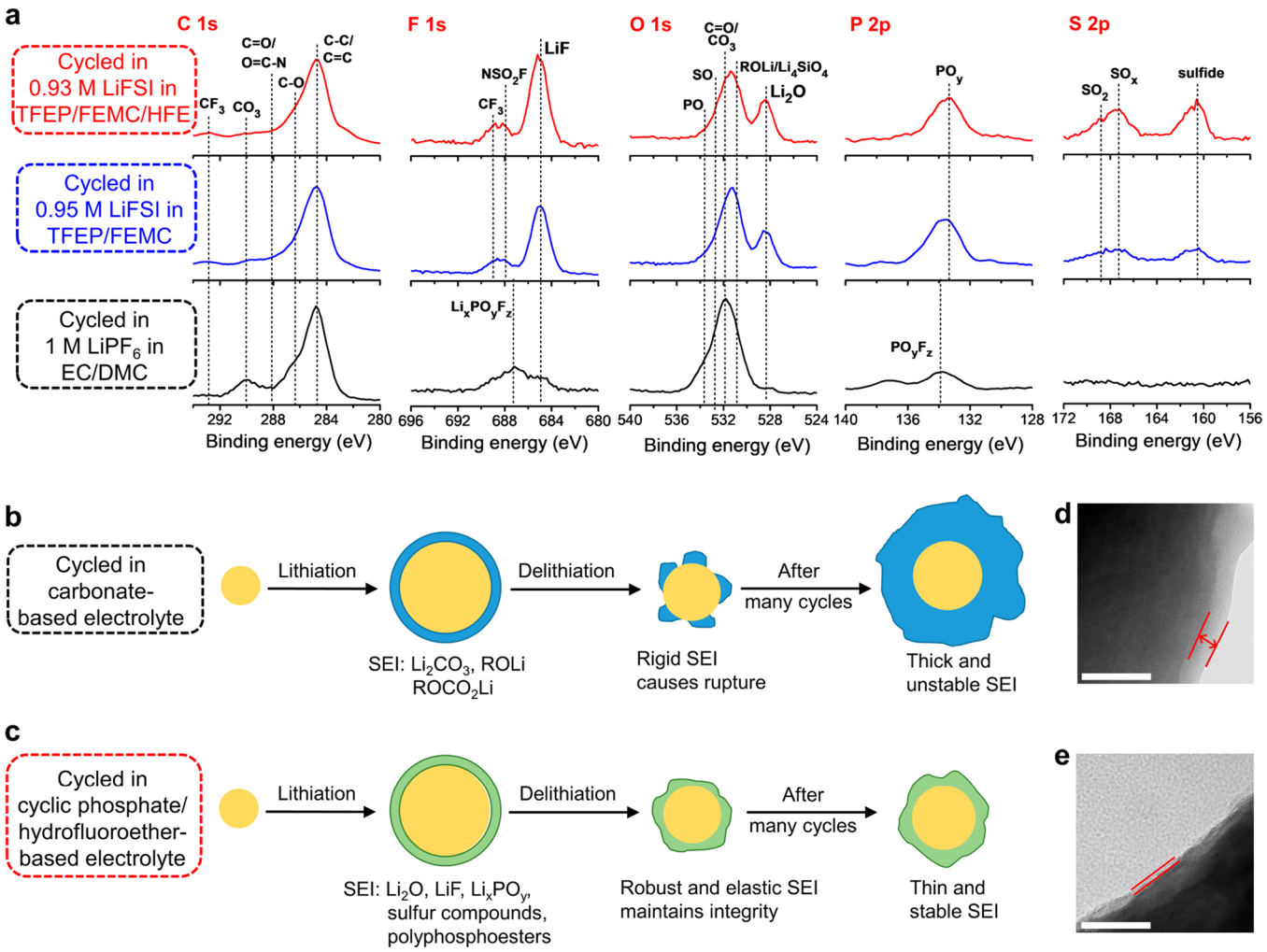

Figure 3. SEIs on SiO electrodes. (a) High-resolution C 1s, F 1s, O 1s, P 2p, and S 2p XPS spectra of SiO electrodes cycled three times in 0.93 M LiFSI in TFEP/FEMC/HFE (red), 0.95 M LiFSI in TFEP/FEMC (blue), and 1 M $LiPF_6$ in EC/DMC (black). Schematic illustrations of SEIs on an SiO particle derived from (b) 1 M $LiPF_6$ in EC/DMC and (c) 0.93 M LiFSI in TFEP/FEMC/HFE. In the conventional EC-based electrolyte, an SEI mainly consisting of Li_2CO_3, $ROCO_2Li$, and ROLi forms at the first lithiation, which is too rigid to tolerate the volumetric stress during delithiation. On the other hand, the SEI generated by the cyclic phosphate/hydrofluoroether-based electrolyte is mainly composed of Li_2O, LiF, Li_xPO_y, sulfur compounds, and polyphosphoesters, which is highly elastic and robust and can sustain the volume changes of SiO upon cycling. TEM images of the SiO electrodes after cycling in (d) 1 M $LiPF_6$ in EC/DMC and (e) 0.93 M LiFSI in TFEP/FEMC/HFE for 100 cycles. The distance between two lines represents the thickness of the SEI, which clearly shows that the SEI formed in 0.93 M LiFSI in TFEP/FEMC/HFE is much thinner than that in 1 M $LiPF_6$ in EC/DMC electrolyte. The white scale bar represents 50 nm.

(99.8%, Figure 2), which has never been achieved for other types of phosphate-based electrolytes, unless they are employed at high concentrations and/or SEI-forming additives are added.[29]

Furthermore, sulfur compounds, including SO_2, SO_x, and sulfide, were detected on the SiO electrodes in both LiFSI electrolytes resulting from the decomposition of LiFSI, where the peak intensities were much stronger for SiO with 0.93 M LiFSI in TFEP/FEMC/HFE. This phenomenon is attributable to the nonsolvating effect of HFE, which intensifies the Li^+–FSI^- association because of the accumulation of CIPs and AGGs. This increases the reduction potential of FSI^- and the proportion of FSI^- anion-derived robust components[55] (mainly sulfur compounds and LiF) in the SEI. In addition, these inorganic components (i.e., LiF, Li_2O, Li_xPO_y, and sulfur compounds) may serve as nanofillers to enhance the mechanical strength of the elastic polymeric components (i.e., polyphosphoesters), thus building a highly elastic and robust inorganic–polymeric SEI (Figure 3c). As shown in the TEM image (Figure 3e) as well as EDS mapping images (Figure S11b), the SiO cycled with 0.93 M LiFSI in TFEP/FEMC/HFE is covered with a very thin and robust SEI layer that is enriched with F, P, O, and S, which can effectively sustain the immense volume changes of microsized SiO upon cycling, enabling the stable cycling of SiO electrodes with a high CE (99.9%, Figure 2).

To further clarify the synergistic effect of TFEP- and FSI^- anion-derived SEI compositions, we first replace the cyclic phosphate TFEP with a common fire-retardant linear phosphate TMP to prepare a LiFSI in TMP/FEMC/HFE electrolyte, with an identical salt-to-solvent molar ratio of 1:8. As shown in Figure S14, the SiO|Li cell using LiFSI in TMP/FEMC/HFE (i.e., without TFEP solvent) delivered an extremely poor cycling performance with fluctuated CE, indicating the failure to produce an effective interphase on the SiO, which in turn suggests the importance of the TFEP

https://doi.org/10.1021/acsenergylett.1c00514
ACS Energy Lett. 2021, 6, 1811–1820

solvent. We then replace the LiFSI with $LiPF_6$ salt to prepare a $LiPF_6$ in TFEP/FEMC/HFE electrolyte, namely, excluding the contribution from FSI^- anion-derived SEI compositions. As shown in Figure S15, the cell using a $LiPF_6$ in TFEP/FEMC/HFE electrolyte retained 51.2% capacity after 200 cycles at 0.2 C, suggesting that the derived SEI can sustain the cycling of microsized Si-based anodes to a certain extent, whereas such an SEI derived from TFEP solvent and $LiPF_6$ salt is not robust enough. Furthermore, $LiPF_6$ suffers from a thermal/chemical instability resulting in the generation of pentafluorophosphorane (PF_5) and hydrogen fluoride (HF), which may decompose the solvents, thereby degrading battery performance. With synergestic contribution from TFEP solvent and FSI^- anion, a highly elastic and robust composite SEI (composed mainly of LiF, Li_2O, Li_xPO_y, sulfur compounds, and polyphosphoesters) was built, which could sustain the immense volume changes of the Si-based anode, as demonstrated by excellent capacity retention and high CE (i.e., 99.9%) in our designed electrolyte (Figure 2), namely, 0.93 M LiFSI in TFEP/FEMC/HFE.

To further demonstrate the superiority of our designed electrolyte, we tested the SiO anode with a high areal mass loading of ~3.5 mg cm^{-2}, corresponding to a high areal capacity of ~5.6 mAh cm^{-2}. As shown in the Figure S16, the SiO|Li cell with 0.93 M LiFSI in TFEP/FEMC/HFE retained 70.7% capacity after 200 cycles at 0.2 C. Furthermore, the designed electrolyte also enables good cycling performance for the microsized Si anode, which suffers from even larger volume expansion (up to 300%). The preliminary Si|Li cell with 0.93 M LiFSI in TFEP/FEMC/HFE maintained 85.2% capacity after 100 cycles, whereas only 5.9% and 50.3% remained after 60 cycles using conventional 1 M $LiPF_6$ in EC/DMC and with 5% FEC additive, respectively (Figure S17).

The Ni-rich NMC622 layered material is one of the standard cathodes for high-energy LIBs. Elevating charging cutoff voltage for layered cathodes dramatically increases its energy density but exacerbates the generation of microcracks, causing structural collapse that disconnects the electrical pathways and significantly deteriorates the electrochemical performance.[9,11,56] Moreover, the safety concerns of Ni-rich cathodes in highly flammable commercial electrolytes have become critical, particularly when they are overcharged and release oxygen that causes thermal runaway and fire hazards.[37,39]

Motivated by our previous work showing that cyclic phosphates can generate a superior polyphosphoester-based CEI on cathodes, as well as an F-rich passivation layer on Al current collectors to suppress Al corrosion,[43] the electrochemical performance of an NMC622 cathode was investigated up to an aggressive cutoff voltage of 4.6 V. As shown in Figure 4, the NMC622|Li cell with 0.93 M LiFSI in TFEP/FEMC/HFE delivered a high initial capacity of ~206 mAh g^{-1}. The initial CE was 86.6%, which reached more than 99% from the second cycle. Notably, the capacity retention was 88.2% after 400 cycles with 99.5% average CE (Figures 4 and S19). This is significantly better than the performance observed with 0.95 M LiFSI in TFEP/FEMC, namely without HFE cosolvent, as well as 1 M $LiPF_6$ in EC/DMC.

As demonstrated in our previous work,[43] 0.95 M LiFSI in TFEP/FEMC formed a F-rich passivation layer (i.e., mainly AlF_3 and LiF) formed on an Al current collector, which could diminish Al corrosion at high potentials to a certain extent. However, pitting on the Al collector was still observed at a high potential of 4.9 V under a harsh polarization time of 48 h (Figure 4c). In contrast, Al corrosion was significantly

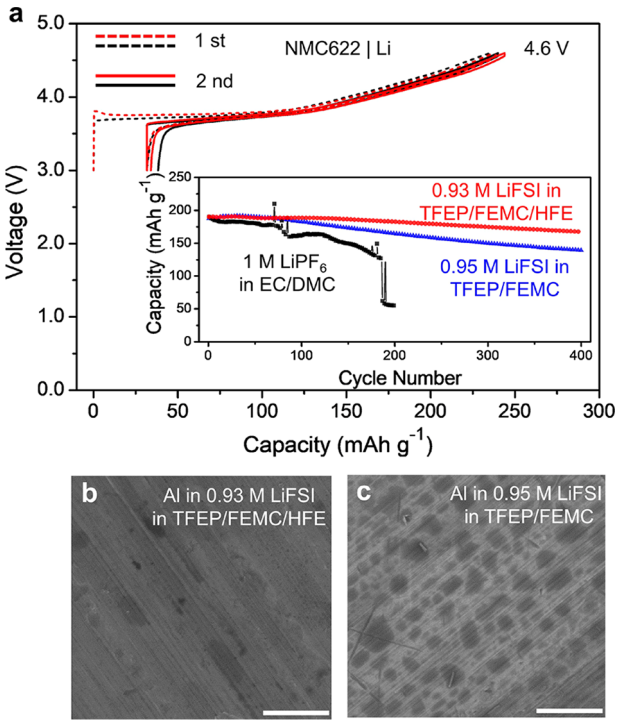

Figure 4. Electrochemical performance of NMC622 cathodes up to 4.6 V. (a) First two charge−discharge profiles of NMC622|Li half-cells with 0.93 M LiFSI in TFEP/FEMC/HFE (red) and 1 M $LiPF_6$ in EC/DMC (black) at a rate of 0.1 C. The inset shows the cycling performance at 0.4 C after three formation cycles at 0.1 C with a cutoff voltage of 3.0−4.6 V. SEM images of the Al foil after the chronoamperometry test at 4.9 V for 48 h in (b) 0.93 M LiFSI in TFEP/FEMC/HFE and (c) 0.95 M LiFSI in TFEP/FEMC. The white scale bar represents 5 μm.

diminished by introducing HFE (Figure 4b), which was ascribed to the fact that the nonsolvating HFE can promote the coordination of TFEP and FEMC to Li^+, thereby reducing free TFEP/FEMC molecules that readily solvate Al^{3+} and cause corrosion.[57] Together with the polyphosphoester-based CEI formed by the ring-opening polymerization of TFEP (Figures S26 and S27), which can suppress electrolyte oxidation and transition-metal dissolution, 0.93 M LiFSI in TFEP/FEMC/HFE electrolyte exhibited an outstanding capability for the operation of Ni-rich cathodes at high cutoff voltages (Figure 4).

After confirmation of the effective passivation on both high-voltage NMC622 cathode and high-capacity SiO anode (Figure 5a), 0.93 M LiFSI in TFEP/FEMC/HFE was investigated for use in an SiO|NMC622 full cell. The SiO anodes were precycled against Li metal at 0.05 C for 2 cycles and then disassembled at a state of charge of 10%. The SiO anodes were then paired with a fresh NMC622 cathode of ~7−8 mg cm^{-2} loading. The full cell showed an initial capacity of ~193 mAh g^{-1} (Figure S21) under a high cutoff voltage of 4.4 V, corresponding to an industrial-level areal capacity of ~1.4 mAh cm^{-2}. The average operating voltage was calculated at 3.50 V, and therefore, the energy density was calculated to be ~590 Wh kg^{-1} based on the total active masses of the cathode and anode, which is a 50−100% improvement compared with the current technologies using $LiCoO_2$ or $LiFePO_4$ as cathodes and graphite as the anode.[1,2]

https://doi.org/10.1021/acsenergylett.1c00514
ACS Energy Lett. 2021, 6, 1811−1820

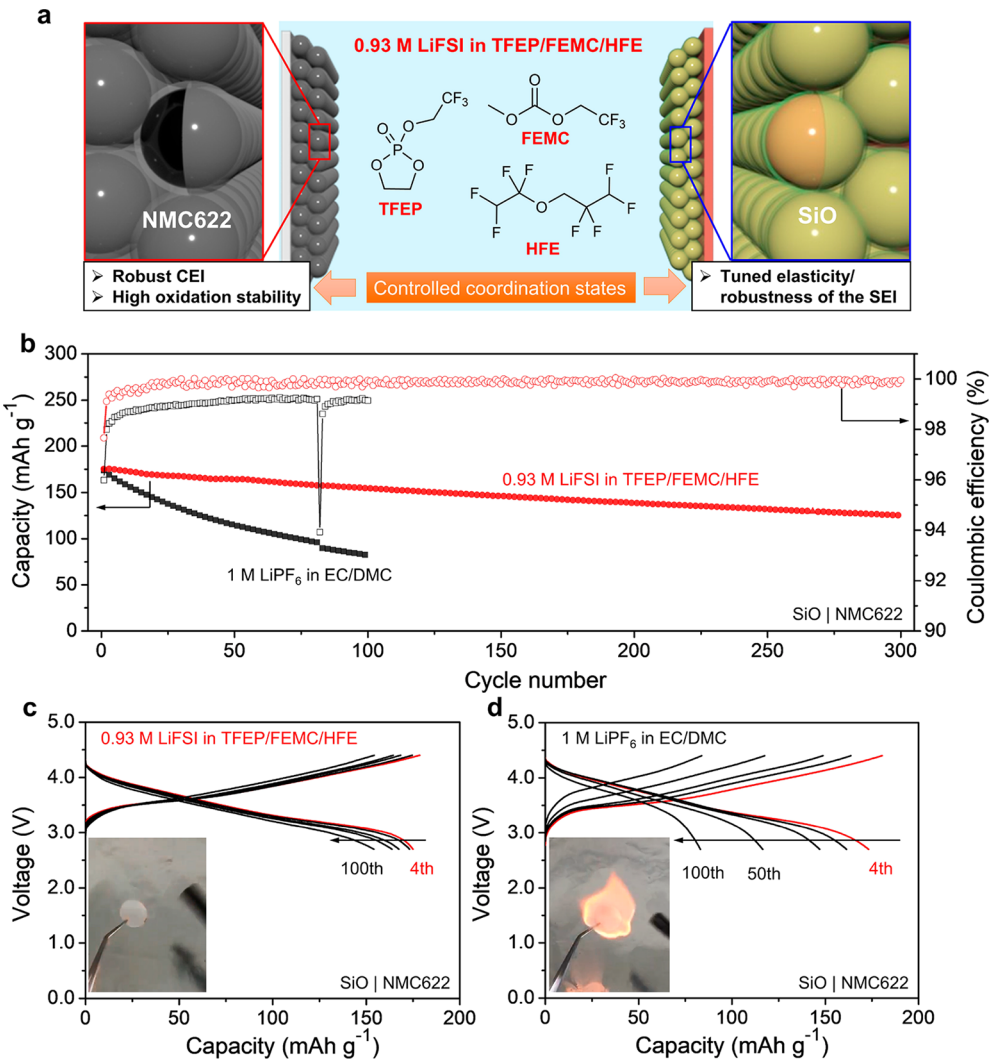

Figure 5. Electrochemical performance of SiO|NMC622 full cells. (a) Schematic illustration of electrolyte composition of 0.93 M LiFSI in TFEP/FEMC/HFE and the battery configuration. The electrolyte is not only completely nonflammable but also able to form robust interphases on both cathode and anode. (b) Discharge capacity and CE of NMC622|SiO full cells with 0.93 M LiFSI in TFEP/FEMC/HFE and conventional 1 M $LiPF_6$ in EC/DMC at 0.4 C after three formation cycles at 0.1 C. Selected charge−discharge curves for the full cells at 0.4 C with (c) 0.93 M LiFSI in TFEP/FEMC/HFE and (d) 1 M $LiPF_6$ in EC/DMC. The capacity is based on the weight of the NMC622 active material. The insets show the flammability test results. The first charge−discharge curves are shown in Figure S21.

The SiO|NMC622 full cell with 0.93 M LiFSI in TFEP/FEMC/HFE exhibited a superior cycling stability, with 71.5% capacity retained and 99.9% average CE obtained after 300 cycles (Figure 5b). Moreover, no obvious increase in voltage polarization was observed (Figure 5c), indicating that the interphases formed on both electrodes remained stable during cycling. The superior performance can be ascribed to the following five reasons: (1) the fluorinated solvents (TFEP, FEMC, and HFE) have significantly high intrinsic oxidative stabilities; (2) the oxidative stability is further enhanced by the strengthened coordination of TFEP and FEMC to Li^+ in the presence of HFE (diluent effect); (3) the Al current collector corrosion in dilute LiFSI solutions is minimized owing to the F-rich passivation layer offered by TFEP and the diluent effect of HFE; (4) the controlled synergistic reduction of TFEP and LiFSI results in a highly elastic and robust composite SEI (composed mainly of LiF, Li_2O, Li_xPO_y, sulfur compounds, and polyphosphoesters) that could sustain the immense volume changes of the Si-based anode; and (5) the ring-opening polymerization of TFEP forms a robust CEI (mainly polyphosphoesters) on the NMC622 cathode (Figures S26 and S27), which not only suppresses electrolyte oxidation but also prevents the dissolution of transition metals, as proved by XPS analysis showing that no transition metals were detected on the surface of the SiO anode as well as inductively coupled plasma optical emission spectrometry (ICP-OES) measurements showing a much lower concentrations of transition-metal ions after 100 cycles (Figures S24 and S25).

In contrast, the cell with 1 M $LiPF_6$ in EC/DMC retained only 47.1% capacity after 100 cycles with a low CE of ~99.0% and exhibited a severe voltage polarization (Figure 5d), which could be attributed to the following three reasons: (1) although Al corrosion can be effectively prevented in 1 M $LiPF_6$ in EC/DMC, the solvent can be easily oxidized when charged over 4.4 V; (2) the electrolyte is continuously reduced on the Si-based anode, resulting in a thick and highly resistive SEI; and (3) the electrolyte fails to produce a CEI on the NMC622 cathode, which thereafter reacts with the HF generated by $LiPF_6$, causing transition-metal ions to dissolve from the cathode and then deposit onto the Si-based anode, as

https://doi.org/10.1021/acsenergylett.1c00514
ACS Energy Lett. 2021, 6, 1811−1820

demonstrated by XPS analysis and ICP-OES results after 100 cycles (Figures S24 and S25).

Thus, in comparison with commercial $LiPF_6$/carbonate electrolytes, the designed electrolyte consisting of 0.93 M LiFSI in TFEP/FEMC/HFE is novel and attractive in several aspects. First, it offers a much wider potential window, which will prompt the application of high-voltage cathodes. Second, the LiFSI salt has favorable thermal/chemical stability as well as a low sensitivity to moisture. Third, it provides a highly elastic and robust SEI that can sustain the immense volume changes of Si-based anodes upon cycling. Fourth, the electrolyte forms a robust CEI on cathodes that can prevent electrolyte oxidation and transition-metal dissolution. Last but not least, the cyclic phosphate-based electrolyte itself is totally nonflammable, which can eliminate potential safety hazards.

In conclusion, we herein rationally designed a nonflammable cyclic phosphate (TFEP)/hydrofluoroether (HFE)-based electrolyte to tune the robustness and elasticity of the SEI on Si-based anodes. The design rationale is that TFEP can form polymeric components, and nonsolvating HFE can intensify the Li^+—FSI^- association to induce additional FSI^- anion-derived inorganic components. This builds a highly elastic and robust composite SEI (mainly LiF, Li_2O, Li_xPO_y, sulfur compounds, and polyphosphoesters), which allows the microsized Si-based particles to undergo elastic deformation and maintain their structural integrity during lithiation—delithiation. Moreover, this electrolyte can also form a polymeric interphase on the cathode side that prevents electrolyte oxidation, transition-metal dissolution, and Al corrosion, thus allowing a Ni-rich NMC622 cathode to operate stably up to a high cutoff voltage of 4.6 V. Our findings shed light on an alternative avenue for designing new electrolytes for aggressive cathode and alloy-based anodes.

■ ASSOCIATED CONTENT

Supporting Information

The Supporting Information is available free of charge at https://pubs.acs.org/doi/10.1021/acsenergylett.1c00514.

Details of experimental methods (including electrolyte and electrode preparation, materials characterization, theoretical calculations, and electrochemical measurements); additional data of Raman spectra, LSV curves, HOMO/LUMO energies, ionic conductivites and viscosities of the electrolytes, CV curves, SEM images, TEM and EDS mapping images, ESI-Q-TOF-MS spectra, electrochemical impedance spectra, and cycling performance (PDF)

■ AUTHOR INFORMATION

Corresponding Authors

Qifeng Zheng − *School of Chemistry, Guangzhou Key Laboratory of Materials for Energy Conversion and Storage, South China Normal University (SCNU), Guangzhou 510006, Guangdong, China;* orcid.org/0000-0003-4330-0903; Email: Qifeng.Zheng@m.scnu.edu.cn

Atsuo Yamada − *Department of Chemical System Engineering, School of Engineering, The University of Tokyo, Tokyo 113-8656, Japan; Elements Strategy Initiative for Catalysts & Batteries (ESICB), Kyoto University, Kyoto 615-8245, Japan;* orcid.org/0000-0002-7880-5701; Email: Yamada@chemsys.t.u-tokyo.ac.jp

Authors

Shaoxiong Yang − *School of Chemistry, Guangzhou Key Laboratory of Materials for Energy Conversion and Storage, South China Normal University (SCNU), Guangzhou 510006, Guangdong, China*

Yuping Zhang − *School of Chemistry, Guangzhou Key Laboratory of Materials for Energy Conversion and Storage, South China Normal University (SCNU), Guangzhou 510006, Guangdong, China*

Zhongliang Li − *School of Chemistry, Guangzhou Key Laboratory of Materials for Energy Conversion and Storage, South China Normal University (SCNU), Guangzhou 510006, Guangdong, China*

Norio Takenaka − *Department of Chemical System Engineering, School of Engineering, The University of Tokyo, Tokyo 113-8656, Japan; Elements Strategy Initiative for Catalysts & Batteries (ESICB), Kyoto University, Kyoto 615-8245, Japan;* orcid.org/0000-0001-7813-4736

Yan Liu − *School of Chemistry, Guangzhou Key Laboratory of Materials for Energy Conversion and Storage, South China Normal University (SCNU), Guangzhou 510006, Guangdong, China*

Hanqin Zou − *School of Chemistry, Guangzhou Key Laboratory of Materials for Energy Conversion and Storage, South China Normal University (SCNU), Guangzhou 510006, Guangdong, China*

Wenting Chen − *Department of Chemical System Engineering, School of Engineering, The University of Tokyo, Tokyo 113-8656, Japan*

Mingcong Du − *School of Chemistry, Guangzhou Key Laboratory of Materials for Energy Conversion and Storage, South China Normal University (SCNU), Guangzhou 510006, Guangdong, China*

Xu-Jia Hong − *School of Chemistry, Guangzhou Key Laboratory of Materials for Energy Conversion and Storage, South China Normal University (SCNU), Guangzhou 510006, Guangdong, China;* orcid.org/0000-0001-9464-9799

Rui Shang − *Department of Chemistry, The University of Tokyo, Tokyo 113-0033, Japan;* orcid.org/0000-0002-2513-2064

Eiichi Nakamura − *Department of Chemistry, The University of Tokyo, Tokyo 113-0033, Japan;* orcid.org/0000-0002-4192-1741

Yue-Peng Cai − *School of Chemistry, Guangzhou Key Laboratory of Materials for Energy Conversion and Storage, South China Normal University (SCNU), Guangzhou 510006, Guangdong, China*

Ya-Qian Lan − *School of Chemistry, Guangzhou Key Laboratory of Materials for Energy Conversion and Storage, South China Normal University (SCNU), Guangzhou 510006, Guangdong, China;* orcid.org/0000-0002-2140-7980

Yuki Yamada − *Department of Chemical System Engineering, School of Engineering, The University of Tokyo, Tokyo 113-8656, Japan; Elements Strategy Initiative for Catalysts & Batteries (ESICB), Kyoto University, Kyoto 615-8245, Japan;* orcid.org/0000-0002-7191-7129

Complete contact information is available at: https://pubs.acs.org/10.1021/acsenergylett.1c00514

Author Contributions

[⊥]S.Y. and Y.Z. contributed equally to this work.

Notes

The authors declare no competing financial interest.

■ ACKNOWLEDGMENTS

This work was supported by JSPS KAKENHI Grant-in-Aid for Scientific Research (No. 20H05673), JST (No. JPMJPF2016), National Natural Science Foundation of China (No. 22005108), Natural Science Foundation of Guangdong Province (No. 2019A1515011460, 2019B1515120027), and Guangdong Science and Technology Department (No. 2020B0101030005, 2021A0505030063).

■ REFERENCES

(1) Armand, M.; Tarascon, J. M. Building better batteries. *Nature* **2008**, *451*, 652.
(2) Li, M.; Lu, J.; Chen, Z.; Amine, K. 30 Years of Lithium-Ion Batteries. *Adv. Mater.* **2018**, *30*, 1800561.
(3) Wu, F.; Maier, J.; Yu, Y. Guidelines and trends for next-generation rechargeable lithium and lithium-ion batteries. *Chem. Soc. Rev.* **2020**, *49*, 1569−1614.
(4) Choi, J. W.; Aurbach, D. Promise and reality of post-lithium-ion batteries with high energy densities. *Nature Reviews Materials* **2016**, *1*, 16013.
(5) Larcher, D.; Tarascon, J. M. Towards greener and more sustainable batteries for electrical energy storage. *Nat. Chem.* **2015**, *7*, 19−29.
(6) Li, W.; Song, B.; Manthiram, A. High-voltage positive electrode materials for lithium-ion batteries. *Chem. Soc. Rev.* **2017**, *46*, 3006−3059.
(7) Xia, Y.; Zheng, J.; Wang, C.; Gu, M. Designing principle for Ni-rich cathode materials with high energy density for practical applications. *Nano Energy* **2018**, *49*, 434−452.
(8) Lee, W.; Muhammad, S.; Sergey, C.; Lee, H.; Yoon, J.; Kang, Y.-M.; Yoon, W.-S. Advances in the Cathode Materials for Lithium Rechargeable Batteries. *Angew. Chem., Int. Ed.* **2020**, *59*, 2578−2605.
(9) Kim, U.-H.; Kim, J.-H.; Hwang, J.-Y.; Ryu, H.-H.; Yoon, C. S.; Sun, Y.-K. Compositionally and structurally redesigned high-energy Ni-rich layered cathode for next-generation lithium batteries. *Mater. Today* **2019**, *23*, 26−36.
(10) Fu, J.; Mu, D.; Wu, B.; Bi, J.; Cui, H.; Yang, H.; Wu, H.; Wu, F. Electrochemical Properties of the LiNi0.6Co0.2Mn0.2O2 Cathode Material Modified by Lithium Tungstate under High Voltage. *ACS Appl. Mater. Interfaces* **2018**, *10*, 19704−19711.
(11) Zhao, Z.; Wen, Z.; Li, C.; Ding, Y.; Jiang, Y.; Wu, F.; Wu, B.; Chen, S.; Mu, D. Effects of different charge cut-off voltages on the surface structure and electrochemical properties of LiNi0.6Co0.2Mn0.2O2. *Electrochim. Acta* **2020**, *353*, 136518.
(12) Tan, S.; Ji, Y. J.; Zhang, Z. R.; Yang, Y. Recent Progress in Research on High-Voltage Electrolytes for Lithium-Ion Batteries. *ChemPhysChem* **2014**, *15*, 1956−1969.
(13) Chen, S.; Wen, K.; Fan, J.; Bando, Y.; Golberg, D. Progress and future prospects of high-voltage and high-safety electrolytes in advanced lithium batteries: from liquid to solid electrolytes. *J. Mater. Chem. A* **2018**, *6*, 11631−11663.
(14) Liu, Z.; Yu, Q.; Zhao, Y.; He, R.; Xu, M.; Feng, S.; Li, S.; Zhou, L.; Mai, L. Silicon oxides: a promising family of anode materials for lithium-ion batteries. *Chem. Soc. Rev.* **2019**, *48*, 285−309.
(15) Chan, C. K.; Peng, H.; Liu, G.; McIlwrath, K.; Zhang, X. F.; Huggins, R. A.; Cui, Y. High-performance lithium battery anodes using silicon nanowires. *Nat. Nanotechnol.* **2008**, *3*, 31−35.
(16) Wu, H.; Chan, G.; Choi, J. W.; Ryu, I.; Yao, Y.; McDowell, M. T.; Lee, S. W.; Jackson, A.; Yang, Y.; Hu, L.; Cui, Y. Stable cycling of double-walled silicon nanotube battery anodes through solid−electrolyte interphase control. *Nat. Nanotechnol.* **2012**, *7*, 310−315.
(17) Li, J.-Y.; Xu, Q.; Li, G.; Yin, Y.-X.; Wan, L.-J.; Guo, Y.-G. Research progress regarding Si-based anode materials towards practical application in high energy density Li-ion batteries. *Materials Chemistry Frontiers* **2017**, *1*, 1691−1708.
(18) Chae, S.; Ko, M.; Kim, K.; Ahn, K.; Cho, J. Confronting Issues of the Practical Implementation of Si Anode in High-Energy Lithium-Ion Batteries. *Joule* **2017**, *1*, 47−60.
(19) Jin, Y.; Zhu, B.; Lu, Z.; Liu, N.; Zhu, J. Challenges and Recent Progress in the Development of Si Anodes for Lithium-Ion Battery. *Adv. Energy Mater.* **2017**, *7*, 1700715.
(20) Rahman, M. A.; Song, G.; Bhatt, A. I.; Wong, Y. C.; Wen, C. Nanostructured Silicon Anodes for High-Performance Lithium-Ion Batteries. *Adv. Funct. Mater.* **2016**, *26*, 647−678.
(21) Li, P.; Hwang, J.-Y.; Sun, Y.-K. Nano/Microstructured Silicon−Graphite Composite Anode for High-Energy-Density Li-Ion Battery. *ACS Nano* **2019**, *13*, 2624−2633.
(22) Eshetu, G. G.; Figgemeier, E. Confronting the Challenges of Next-Generation Silicon Anode-Based Lithium-Ion Batteries: Role of Designer Electrolyte Additives and Polymeric Binders. *ChemSusChem* **2019**, *12*, 2515−2539.
(23) Yang, H. S.; Kim, S.-H.; Kannan, A. G.; Kim, S. K.; Park, C.; Kim, D.-W. Performance Enhancement of Silicon Alloy-Based Anodes Using Thermally Treated Poly(amide imide) as a Polymer Binder for High Performance Lithium-Ion Batteries. *Langmuir* **2016**, *32*, 3300−3307.
(24) Huang, Q.; Song, J.; Gao, Y.; Wang, D.; Liu, S.; Peng, S.; Usher, C.; Goliaszewski, A.; Wang, D. Supremely elastic gel polymer electrolyte enables a reliable electrode structure for silicon-based anodes. *Nat. Commun.* **2019**, *10*, 5586.
(25) Choi, S.; Kwon, T.-w.; Coskun, A.; Choi, J. W. Highly elastic binders integrating polyrotaxanes for silicon microparticle anodes in lithium ion batteries. *Science* **2017**, *357*, 279−283.
(26) Kim, K.; Ma, H.; Park, S.; Choi, N.-S. Electrolyte-Additive-Driven Interfacial Engineering for High-Capacity Electrodes in Lithium-Ion Batteries: Promise and Challenges. *ACS Energy Letters* **2020**, *5*, 1537−1553.
(27) Chae, S.; Kwak, W.-J.; Han, K. S.; Li, S.; Engelhard, M. H.; Hu, J.; Wang, C.; Li, X.; Zhang, J.-G. Rational Design of Electrolytes for Long-Term Cycling of Si Anodes over a Wide Temperature Range. *ACS Energy Letters* **2021**, *6*, 387−394.
(28) Jaumann, T.; Balach, J.; Langklotz, U.; Sauchuk, V.; Fritsch, M.; Michaelis, A.; Teltevskij, V.; Mikhailova, D.; Oswald, S.; Klose, M.; Stephani, G.; Hauser, R.; Eckert, J.; Giebeler, L. Lifetime vs. rate capability: Understanding the role of FEC and VC in high-energy Li-ion batteries with nano-silicon anodes. *Energy Storage Materials* **2017**, *6*, 26−35.
(29) Zeng, Z.; Liu, X.; Jiang, X.; Liu, Z.; Peng, Z.; Feng, X.; Chen, W.; Xia, D.; Ai, X.; Yang, H.; Cao, Y. Enabling an intrinsically safe and high-energy-density 4.5 V-class Li-ion battery with nonflammable electrolyte. *InfoMat* **2020**, *2*, 984−992.
(30) Matsumoto, K.; Inoue, K.; Utsugi, K. A highly safe battery with a non-flammable triethyl-phosphate-based electrolyte. *J. Power Sources* **2015**, *273*, 954−958.
(31) Nguyen, D.-T.; Kang, J.; Nam, K.-M.; Paik, Y.; Song, S.-W. Understanding interfacial chemistry and stability for performance improvement and fade of high-energy Li-ion battery of LiNi0.5-Co0.2Mn0.3O2//silicon-graphite. *J. Power Sources* **2016**, *303*, 150−158.
(32) Sina, M.; Alvarado, J.; Shobukawa, H.; Alexander, C.; Manichev, V.; Feldman, L.; Gustafsson, T.; Stevenson, K. J.; Meng, Y. S. Direct Visualization of the Solid Electrolyte Interphase and Its Effects on Silicon Electrochemical Performance. *Adv. Mater. Interfaces* **2016**, *3*, 1600438.
(33) Jin, Y.; Kneusels, N.-J. H.; Marbella, L. E.; Castillo-Martínez, E.; Magusin, P. C. M. M.; Weatherup, R. S.; Jónsson, E.; Liu, T.; Paul, S.; Grey, C. P. Understanding Fluoroethylene Carbonate and Vinylene Carbonate Based Electrolytes for Si Anodes in Lithium Ion Batteries with NMR Spectroscopy. *J. Am. Chem. Soc.* **2018**, *140*, 9854−9867.
(34) Chen, J.; Fan, X.; Li, Q.; Yang, H.; Khoshi, M. R.; Xu, Y.; Hwang, S.; Chen, L.; Ji, X.; Yang, C.; He, H.; Wang, C.; Garfunkel, E.; Su, D.; Borodin, O.; Wang, C. Electrolyte design for LiF-rich solid−electrolyte interfaces to enable high-performance microsized alloy anodes for batteries. *Nature Energy* **2020**, *5*, 386−397.

https://doi.org/10.1021/acsenergylett.1c00514
ACS Energy Lett. 2021, 6, 1811−1820

(35) Roth, E. P.; Orendorff, C. J. How Electrolytes Influence Battery Safety. *Electrochem. Soc. Interface* **2012**, *21*, 45−49.
(36) Rodrigues, M.-T. F.; Babu, G.; Gullapalli, H.; Kalaga, K.; Sayed, F. N.; Kato, K.; Joyner, J.; Ajayan, P. M. A materials perspective on Li-ion batteries at extreme temperatures. *Nature Energy* **2017**, *2*, 17108.
(37) Wu, X.; Song, K.; Zhang, X.; Hu, N.; Li, L.; Li, W.; Zhang, L.; Zhang, H. Safety Issues in Lithium Ion Batteries: Materials and Cell Design. *Front. Energy Res.* **2019**, *7*, 65 DOI: 10.3389/fenrg.2019.00065.
(38) Dokko, K.; Tachikawa, N.; Yamauchi, K.; Tsuchiya, M.; Yamazaki, A.; Takashima, E.; Park, J.-W.; Ueno, K.; Seki, S.; Serizawa, N.; Watanabe, M. Solvate Ionic Liquid Electrolyte for Li−S Batteries. *J. Electrochem. Soc.* **2013**, *160*, A1304−A1310.
(39) Duan, J.; Tang, X.; Dai, H.; Yang, Y.; Wu, W.; Wei, X.; Huang, Y. Building Safe Lithium-Ion Batteries for Electric Vehicles: A Review. *Electrochemical Energy Reviews* **2020**, *3*, 1−42.
(40) Izquierdo-Gonzales, S.; Li, W.; Lucht, B. L. Hexamethylphosphoramide as a flame retarding additive for lithium-ion battery electrolytes. *J. Power Sources* **2004**, *135*, 291−296.
(41) Zeng, Z.; Wu, B.; Xiao, L.; Jiang, X.; Chen, Y.; Ai, X.; Yang, H.; Cao, Y. Safer lithium ion batteries based on nonflammable electrolyte. *J. Power Sources* **2015**, *279*, 6−12.
(42) Wang, J.; Yamada, Y.; Sodeyama, K.; Watanabe, E.; Takada, K.; Tateyama, Y.; Yamada, A. Fire-extinguishing organic electrolytes for safe batteries. *Nature Energy* **2018**, *3*, 22−29.
(43) Zheng, Q.; Yamada, Y.; Shang, R.; Ko, S.; Lee, Y.-Y.; Kim, K.; Nakamura, E.; Yamada, A. A cyclic phosphate-based battery electrolyte for high voltage and safe operation. *Nature Energy* **2020**, *5*, 291−298.
(44) Nifant'ev, I. E.; Shlyakhtin, A. V.; Bagrov, V. V.; Komarov, P. D.; Kosarev, M. A.; Tavtorkin, A. N.; Minyaev, M. E.; Roznyatovsky, V. A.; Ivchenko, P. V. Controlled ring-opening polymerisation of cyclic phosphates, phosphonates and phosphoramidates catalysed by heteroleptic BHT-alkoxy magnesium complexes. *Polym. Chem.* **2017**, *8*, 6806−6816.
(45) Moon, H.; Mandai, T.; Tatara, R.; Ueno, K.; Yamazaki, A.; Yoshida, K.; Seki, S.; Dokko, K.; Watanabe, M. Solvent Activity in Electrolyte Solutions Controls Electrochemical Reactions in Li-Ion and Li-Sulfur Batteries. *J. Phys. Chem. C* **2015**, *119*, 3957−3970.
(46) Yamada, Y.; Furukawa, K.; Sodeyama, K.; Kikuchi, K.; Yaegashi, M.; Tateyama, Y.; Yamada, A. Unusual Stability of Acetonitrile-Based Superconcentrated Electrolytes for Fast-Charging Lithium-Ion Batteries. *J. Am. Chem. Soc.* **2014**, *136*, 5039−5046.
(47) Takada, K.; Yamada, Y.; Yamada, A. Optimized Nonflammable Concentrated Electrolytes by Introducing a Low-Dielectric Diluent. *ACS Appl. Mater. Interfaces* **2019**, *11*, 35770−35776.
(48) Chen, S.; Zheng, J.; Mei, D.; Han, K. S.; Engelhard, M. H.; Zhao, W.; Xu, W.; Liu, J.; Zhang, J.-G. High-Voltage Lithium-Metal Batteries Enabled by Localized High-Concentration Electrolytes. *Adv. Mater.* **2018**, *30*, 1706102.
(49) Ren, X.; Chen, S.; Lee, H.; Mei, D.; Engelhard, M. H.; Burton, S. D.; Zhao, W.; Zheng, J.; Li, Q.; Ding, M. S.; Schroeder, M.; Alvarado, J.; Xu, K.; Meng, Y. S.; Liu, J.; Zhang, J.-G.; Xu, W. Localized High-Concentration Sulfone Electrolytes for High-Efficiency Lithium-Metal Batteries. *Chem.* **2018**, *4*, 1877−1892.
(50) Chen, S.; Zheng, J.; Yu, L.; Ren, X.; Engelhard, M. H.; Niu, C.; Lee, H.; Xu, W.; Xiao, J.; Liu, J.; Zhang, J.-G. High-Efficiency Lithium Metal Batteries with Fire-Retardant Electrolytes. *Joule* **2018**, *2*, 1548.
(51) Zhang, Z.; Hu, L.; Wu, H.; Weng, W.; Koh, M.; Redfern, P. C.; Curtiss, L. A.; Amine, K. Fluorinated electrolytes for 5 V lithium-ion battery chemistry. *Energy Environ. Sci.* **2013**, *6*, 1806−1810.
(52) Nie, M.; Chalasani, D.; Abraham, D. P.; Chen, Y.; Bose, A.; Lucht, B. L. Lithium Ion Battery Graphite Solid Electrolyte Interphase Revealed by Microscopy and Spectroscopy. *J. Phys. Chem. C* **2013**, *117*, 1257−1267.
(53) Cui, C.; Yang, C.; Eidson, N.; Chen, J.; Han, F.; Chen, L.; Luo, C.; Wang, P.-F.; Fan, X.; Wang, C. A Highly Reversible, Dendrite-Free Lithium Metal Anode Enabled by a Lithium-Fluoride-Enriched Interphase. *Adv. Mater.* **2020**, *32*, 1906427.
(54) Chen, T.; Wu, J.; Zhang, Q.; Su, X. Recent advancement of SiOx based anodes for lithium-ion batteries. *J. Power Sources* **2017**, *363*, 126−144.
(55) Yamada, Y.; Yamada, A. Superconcentrated Electrolytes to Create New Interfacial Chemistry in Non-aqueous and Aqueous Rechargeable Batteries. *Chem. Lett.* **2017**, *46*, 1056−1064.
(56) Schipper, F.; Erickson, E. M.; Erk, C.; Shin, J.-Y.; Chesneau, F. F.; Aurbach, D. Review—Recent Advances and Remaining Challenges for Lithium Ion Battery Cathodes. *J. Electrochem. Soc.* **2017**, *164*, A6220−A6228.
(57) Yamada, Y.; Chiang, C. H.; Sodeyama, K.; Wang, J.; Tateyama, Y.; Yamada, A. Corrosion Prevention Mechanism of Aluminum Metal in Superconcentrated Electrolytes. *ChemElectroChem* **2015**, *2*, 1687−1694.

https://doi.org/10.1021/acsenergylett.1c00514
ACS Energy Lett. 2021, 6, 1811−1820